Journal of Basic and Environmental Sciences 3 (2016) 123– 132 **ISSN 2356-6388**

Research Article ***Open Access***

Kinetics and isotherm studies of Remazol Red adsorption onto polyaniline/ cerium oxide nanocomposites

M. Khairy*[a], R. Kamal[b], N. H. Amin[b], M. A. Mousa[a]

[a]Chemistry Department, Faculty of Science, Benha University, Benha, Egypt.
[b]Chemistry Department, Faculty of Education, Ain shams University, Roxy 11757, Cairo, Egypt.
* Corresponding author. Tel.: +20201270405481, +9660502508917.
E-mail address: Khairy_m22@yahoo.com

Received: 20 Aug. 2016, In Revised form; 3 Sept. 2016, Accepted 3 Sept. 2016, Available online 1 Oct. 2016

Abstract:
Polyaniline/cerium oxide (PANI/CeO_2) composites were prepared and characterized by XRD, FT-IR, nitrogen adsorption/desorption isotherms and TEM techniques. The PANI/CeO_2 composites were used for removal of Remazol Red (RB-133) from aqueous solution. The adsorption behaviour of dye was studied at different experimental conditions of solution pH and reaction temperature. The adsorption isotherm studies were carried out using Langmuir and Freundlich models, of which Freundlich model was found more suitable. Pseudo-second-order model fitted well with good agreement with the experimental values of q_e (equilibrium adsorption capacity). Thermodynamic parameters for the adsorption system were calculated and suggested that the adsorption process is spontaneous, exothermic and marked with an increase in randomness at the solid–liquid interface.

Keywords: Polyaniline; polyaniline/ cerium oxide; Remazol red dye; Adsorption isotherm.

1. Introduction

Nowadays, Many industries are produced large amounts of organic dyes and also used in in textile, papers, dyestuffs, plastic, pharmaceutical and food industries. However, Dye materials are important sources of the environmental contaminations due to their non-bio degradability and high toxicity to aquatic creatures and carcinogenic effects on humans [1]. The presence of very small amounts of dyes in water is highly visible and affects the quality of water. Moreover, it is very difficult to degrade dyes because they are stable to light, heat and oxidizing agents.

Dyes can be divided according to the chemical nature into: acridine dyes, azo dyes, arylmethane dyes, anthraquinone dyes, nitro dyes, etc. azo dyes are the largest chemical class of dyes which have been used extensively in textile industries due to their low cost, stability and variety of colors [2]. Removal of these dyes from wastewater is difficult because of their high solubility in water, synthetic origin and mainly aromatic structures, which are biologically non-degradable. several physical, chemical and biological decolorization techniques have been applied to remove dyes from wastewater, such as photochemical degradation, biological degradation, coagulation, chemical oxidation, reverse osmosis, flotation and adsorption. Among these techniques, adsorption process is commonly used and gives the best results owing to its high efficiency and ability to remove different types of coloring materials, simplicity of design, low-cost and economic feasibility [3-9].

A few productive and particular adsorbent materials have been created, for example, waste orange peel, banana substance, rice husk, clay, and activated carbon [10-12] . Recently, a conducting polymer, polyaniline (PANI), was tested in the adsorption of dye effluent [13]. Polyaniline is thought to be a standout amongst the most encouraging classes of natural directing polymers because of their all around characterized electrochemistry, simple protonation reversibility, fabulous redox recyclability, and good environmental stability, and variety of nanostructured morphologies. PANI usually combined with inorganic materials to form composites with high physical, mechanical, and electrical properties, etc. In recent years, rare earth oxides are introduced into the preparation of polyaniline composites because of their excellent physical and chemical characteristics. Among those oxides, CeO_2 has potential applications in various fields including catalysis and coatings. The high thermal resistance and inflexibility of its structure make CeO_2 an important material for several technologies [14].

The present study is an attempt to remove the anionic dye Remazol Red RB-133 (RR RB-133), as a model dye, from aqueous solutions by using each of polyaniline and polyaniline/CeO_2 nano composites with various compositions (1 and 5 wt% CeO_2) as adsorbents. Physical properties of the adsorbent materials besides the kinetics and the adsorption isotherms were also investigated.

2. Experimental

2.1. Preparation of CeO_2 nanoparticles

A cerium oxide powder was prepared by low-temperature combustion synthesis method in the presence of chelating agent citric acid [15]. The molar ratio of $Ce(NO_3)_3.6H_2O$: citric acid of 1:1 were dissolved completely in de-ionized water and the pH value of the solution was adjusted to be 7. The mixture solution was stirred well using a magnetic stirrer for about 2 h and then, the prepared mixture solution was reflux at a temperature of 80°Cfor about 4 h. the sol heated at 80°C for 12h. The obtained pale-yellow powder was calcined in furnace at 750 °C for 1.5 h.

2.2. Preparation of polyaniline

Polyaniline was synthesized by chemical polymerization using ammonium persulfate (APS) as oxidant and HNO_3 as doping agent, respectively [16]. 1.6 mL of aniline was 50 mL dissolved in 100 mL of 1 M HNO_3 aqueous solutions. While maintaining vigorous stirring within ice temperature (0 – 5 ºC), APS (4.564 g) in 100 mL of dist. H_2O was rapidly poured into the aniline solution. The mixture was stirred at this temperature for 10 h. At the end, the product was collected by filtration and washed with DI water and then acetone several times, until the filtrate became colorless. After drying in oven at 70 ºC and sieving for 12 h, the PANI was obtained as a powder.

2.3. Preparation of Polyaniline/CeO_2 composites

The polyaniline/CeO_2 composites were prepared by in situ polymerization of aniline in a suspension of CeO_2 particles in acidic solution. The content of CeO_2 (wt%) doped into aniline was fixed at 1%, 3% and 5%, respectively. Typically, 1.6 mL aniline was dissolved in 100 mL of 1 M HNO_3 containing CeO_2 powder under ultrasonic action. After 1 h, while maintaining vigorous stirring within ice temperature (0 – 5 ºC), APS (4.564 g) in 100 mL of dist. H_2O was rapidly poured into the aniline solution. The mixture was stirred at this temperature for 10 h. At the end, the precipitated powder was filtered and washed with DI water and then acetone several times, until the filtrate became colorless. After drying in oven at 70 ºC and sieving for 12 h. The resulting nanocomposites with respect to different CeO_2 amounts of 1 and 5 wt% are denoted as PANI/CeO_2-1 and PANI/CeO_2-5 respectively.

2.4. Characterization

X-ray diffraction (XRD) patterns, obtained on an X-ray diffractometer (type Bruker Axs D8 Advance, Germany) using CuKα1 irradiation (λ = 0.15404 Å) at a scan rate of 2° in 2θ/min, were used to determine the identity of any phase present and their crystallite size. Fourier transform infrared (FT-IR) spectroscopy of composites was recorded on a Jasco FT-IR 4100 spectrometer (Japan) using KBr pellets in the range of 4000–400 cm^{-1} region. The surface characteristics, namely specific surface areas (S_{BET}), total pore volume (V_p) and average pore radius (ŕ) of the various catalysts were determined from nitrogen adsorption isotherms measured at −196 °C using a Quanta chrome NOVA 2000 automated gas-sorption apparatus model 7.11 (USA). All catalysts were degassed at 200 °C for 2 h under a reduced pressure of 1.3 mPa before taking the measurements. Morphology of the samples was investigated using transmission electron microscope (TEM) (JEM-2100CX (JEOL)).

2.5. Adsorption studies

The adsorption of water-soluble reactive dye Remazol Red RB- 133 (RR RB-133) from aqueous solution onto the adsorbents was performed using batch equilibrium technique. All the experiments were carried out at 25 °C. For the determination of adsorption isotherms, 100 mL of dye solution of known initial concentration was shaken with a certain amount of the adsorbent (100 mg) on a stirrer at 25 °C and pH = 6.5. Initial dye concentrations were changed in the range of 25 mg L^{-1} to 75 mg L^{-1}. At various time intervals, samples were taken and allowed to settle and further centrifuged at 7000 rpm for 10 min. The concentration of the residual dye was measured using UV–vis spectrophotometer (Jasco V-550, Japan) at appropriate wavelength corresponding to the maximum absorption of Remazol Red RB-133 (i.e., 520 nm). This data was used to calculate the adsorption capacity of the adsorbent. Initial dye concentration in the solution was varied to investigate its effect on the adsorption capacity. The equilibrium adsorption capacities (qe) were then obtained by using the following mass balance equation.

$$q_e = (C_0 - C_e)\frac{V}{W} \qquad (1)$$

Where q_e is the adsorption capacity (dye adsorbed onto the mass unit of the sample, mg/g), Where C_o and C_e are the initial and equilibrium dye concentrations in solution (mg/L) respectively, W is the adsorbent amount (g), and V is the volume of solution (L). Adsorption isotherms were investigated by Langmuir and Freundlich models. The reaction kinetics were performed by pseudo-first-order kinetic model, pseudo-second-order kinetic model and intra-particle diffusion model.

3. Results and discussions

3.1. Characterization of adsorbents

3.1.1. XRD

Fig. 1 shows the XRD pattern of synthesized CeO_2 nanoparticles, pure PANI and PANI/CeO_2-5 nanocomposite. Fig. 1a shows the XRD pattern of CeO_2 nanoparticles synthesized by combustion method. All the diffraction peaks of CeO_2 are indexed to cerianite-(Ce): syn structure with cubic phase, lattice points a=b=c=5.41134 Å, space group: Fm-3m (no. 225) and Joint Committee on Powder Diffraction Standards (JCPDS) no. 34-0394 [17]. The powder XRD pattern of CeO_2 nanoparticles had shown broad peaks, which confirmed the formation of small-sized nanoparticles. The particle size of nanoparticles are determined using the Scherrer's relation: $d = (0.9\lambda)/(\beta\cos\theta)$ [18], where is β the full width at half maximum in radians, λ is the wavelength of X-rays used, and θ is the Bragg's angle. The average

crystallite size calculated from the most intense peaks (2θ=28.5 º) by the Scherrer formula was found to be 35 nm. Further, Fig. 1b shows the XRD pattern of PANI which exhibits broad peaks at 2θ = 15.2◦, 21.5◦ and 25.3◦. The XRD pattern of PANI/CeO_2-5 nanocomposite is showed in Fig. 1c.It exhibited the same pattern as obtained in the pure CeO_2, representing that the crystal structure of CeO_2 is not altered by the PANI chain. Besides, some extra peaks observed in nanocomposite may be assignable to the dopants of PANI chain. Furthermore, these results demonstrate that PANI is amorphous in the nanocomposite, which suggest that the addition of CeO_2 nanoparticles hinders the crystallization of the PANI chain. This confirms that the PANI/CeO_2-5 nanocomposite has become more crystalline as the concentration of CeO_2 is increased and PANI deposited on the surface of CeO_2 nanoparticles has no effect on the crystallization behavior of CeO_2 nanoparticles in the nanocomposite [19].

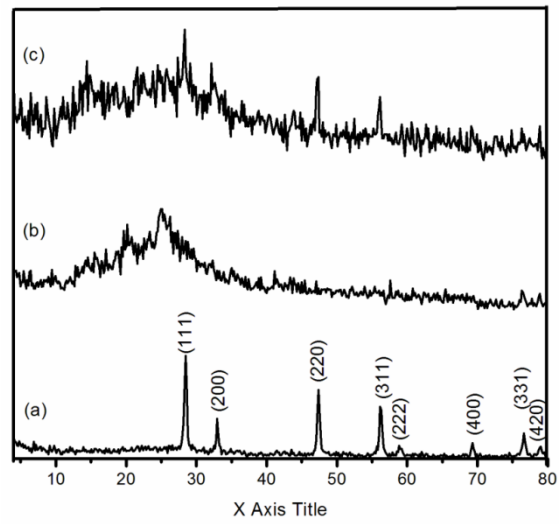

Fig. 1 XRD spectra of (a) CeO_2 nanoparticles, (b) PANI and (c) PANI/CeO_2-5nanocomposite.

3.1.2. FT-IR

Fig. 2 shows the FTIR spectra of CeO_2, PANI and PANI/CeO_2-5 nanocomposite specimens. The spectrum of CeO_2, Fig. 3a, shows bands at 563 and 829 cm^{-1} which are ascribed to (Ce–O) metal–oxygen vibrations [20]**.** Polymerization of aniline can be confirmed by the presence of spectral bands at 1476 and 1563 cm^{-1}, Fig. 2b, which are recognized to stretching of the benzenoid and quinoid rings, respectively, for the HNO_3 doped PANI. These results point to that the pure PANI is highly doped and exists in conducting emeraldine salt form [21]. The band observed at 1300 cm^{-1} matching to C–N stretching of secondary amine in the polymer main chain. The FT-IR spectrum of the PANI/CeO_2-5 nanocomposite (Fig. 2c) shows bands related to both the polyaniline (quinoid and benzenoid rings at 1562 and 1471 cm^{-1}, respectively, and CeO_2 nanoparticles (at 583 cm^{-1}) besides a band at 3436 cm^{-1} ascribed to N–H stretching vibrations bending mode. The specific bands observed for the polyaniline functional groups are seen at somewhat higher frequency than their actual value owing to their interaction with CeO_2 nanoparticles. Really, there are several types of interactions may occur between the polyhedral groups of CeO_2 nanoparticles with the polymeric ring of polyaniline causing the observed shift e.g. the interaction between a lone pair of electrons of nitrogen atom with the above mentioned groups [22].

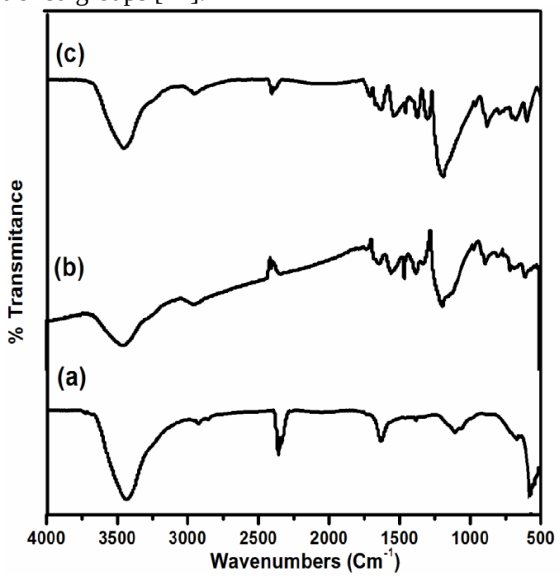

Figure 2. FT-IR spectra of (a) CeO_2 nanoparticles, (b) PANI and (c) PANI/CeO_2-5 nanocomposite.

3.1.3. Specific surface areas and porosity

Fig. 3 displays the nitrogen adsorption–desorption isotherms of CeO_2, PANI and PANI/CeO_2 nanocomposites. The nitrogen sorption isotherms of all specimens are similar and belong to the type IV of Brunauer's classifications with closed hysteresis loops of type H3, demonstrating the formation of mesoporous structures. The specific surface areas were calculated using the BET (Brunauer–Emmett–Teller) method [23] and the results obtained are recorded in Table 1. From which it can be seen that the surface area increases with increasing of CeO_2 content in the composite. This might be due to an incorporation of oxide particles in the polymeric structure of polyaniline forming voids between the particles. The total pore volumes, V_P, were taken at P/P° = 0.95 and was found to be lying in the scope of 0.31–0.42 ml/g. The pore radius was calculated and extended from 15.1–19.8 nm showing the formation of narrow mesoporous structure, Table 1.

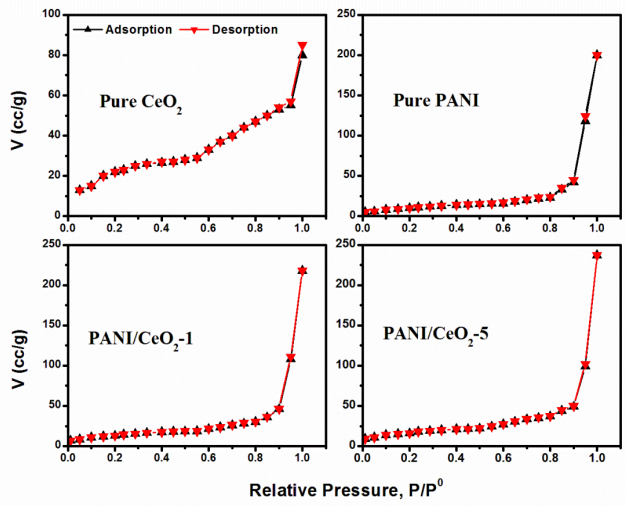

Fig. 3 Nitrogen adsorption–desorption isotherms of (a) CeO_2 and PANI/CeO_2 nanocomposites with (b) 1 wt%, (c) 5 wt% of CeO_2.

Table 1 Surface parameters of CeO_2, PANI and PANI/CeO_2 nanocomposites.

samples	S_{BET} (m^2/g)	V_p(mL/g)	ŕ (nm)
CeO_2	70	0.42	15.1
PANI	39	0.31	19.8
PANI/CeO_2-1	49	0.34	17.0
PANI/CeO_2-5	60	0.36	15.3

3.1.4. Morphology

Morphological studies were done with TEM, which confirm the formation of nanocomposite. Fig. 4 shows the TEM images of CeO_2, PANI and PANI/CeO_2-5 nanocomposite. The TEM image of CeO_2, Fig. 4a, illustrates different sizes of round molded CeO_2 particles with slight agglomeration. And the TEM image of PANI, Fig. 4b, shows short fibers with diverse size. Whereas, TEM image of PANI/CeO_2-5 nanocomposite demonstrates great scattering of circular particles of CeO_2 in the aggregate of PANI chains, Fig. 4c. Comparing the TEM images show the growing of PANI on theCeO_2 nanoparticle surfaces. Polyaniline layers on the CeO_2 nanoparticle surface attached together and generated the porous PANI/CeO_2 nanocomposite.

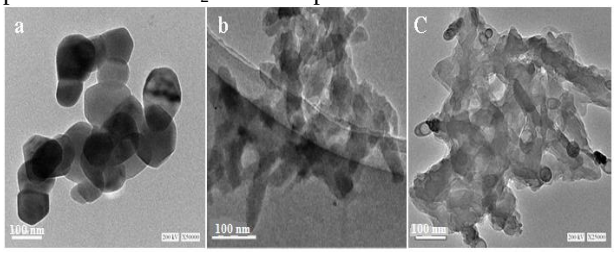

Fig. 4 TEM image of (a) CeO_2 nanoparticles, (b) PANI and (c) PANI/CeO_2-5 nanocomposite.

3.2. Effect of various parameters on adsorption

In the present study, PANI/CeO_2-5 was used for Remazol Red RB-133 (RR RB- 133) removal from aqueous solutions. The effect of various important parameters such as solution pH and reaction temperature were investigated.

3.2.1. Effect of pH

The pH of the solution affects the surface charge of the adsorbent and also the degree of ionization of the materials present in the solution. Increase in the solution pH causes the dissociation of the functional groups on the adsorbent surface active sites which in turn affects the adsorptive process. For studying the effect of pH on the adsorption performance was studied by conducting the batch experiments for 50 mg L^{-1} dye solutions of different initial pH values (2.0–10.0). The experiment was done with 0.1 g of nano PANI/CeO_2-5 at 25 ºC. The pH of solutions were adjusted by 0.1 mol L^{-1} HNO_3 or 0.1 mol L^{-1} NaOH. Fig. 5 shows the variation of adsorption capacity of nano PANI/CeO_2-5 at different pH values. As seen from the graph, the equilibrium adsorption capacity increases with increase in pH, reaches maximum at pH 6.5 and then decreases. The lower q_e values in basic pH may be due to slight dissolution of PANI–CeO_2, while higher q_e the surface charge of PANI/CeO_2 and dye molecules. The charge of the dye molecules is highly negative due to the presence of four SO_3^-groups on each molecule. Electrostatic forces of attraction between the positively charged PANI/CeO_2 and negatively charged remazol Red RB-133 is responsible for the high adsorption capacity observed below pH 8.0. However, a drastic decrease in the dye removal efficiency is observed in basic conditions which might be due to the formation of hydroxyl ions and subsequent competition with the dye molecules for adsorption active sites [24 - 26].

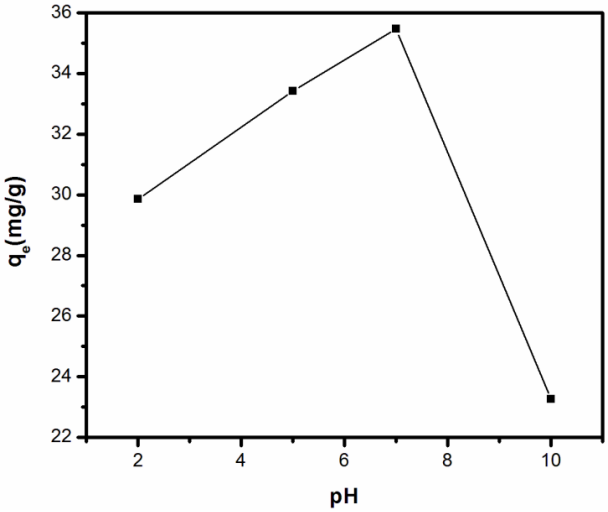

Fig. 5 Effect of pH on the adsorption capacity of PANI/CeO_2-5 nanocomposite toward Remazol Red RB-133 (dye concentration is 50 mg L^{-1}, adsorbent dosage = 0.1 g L^{-1}).

3.2.2. Effect of temperature

The effect of temperature on the sorption of 50 mgL^{-1} Remazol Red RB-133 on PANI/CeO_2-5 nanocomposite was studied by performing the adsorption experiments at different temperatures (25, 35, 45 and 55 ºC). The results

revealed that the adsorption capacity decreased with increase in temperature from 25 to 55 ºC (Fig. 6) and maximum adsorption capacity is noticed at 25 ºC which shows an exothermic nature of dye adsorption. The decrease in the rate of adsorption with the increase in temperature may be attributed to the physical bonding between acid dye molecules and the active sites of the adsorbent. It is weakened as temperature increased, whereas, the solubility of dyes increased thus interaction forces between the solute and the solvent become stronger than those between solute and adsorbent, making the solute more difficult to adsorb. The adsorption is favored by a decrease in temperature, a phenomenon which is also characteristic of physical adsorption [27].

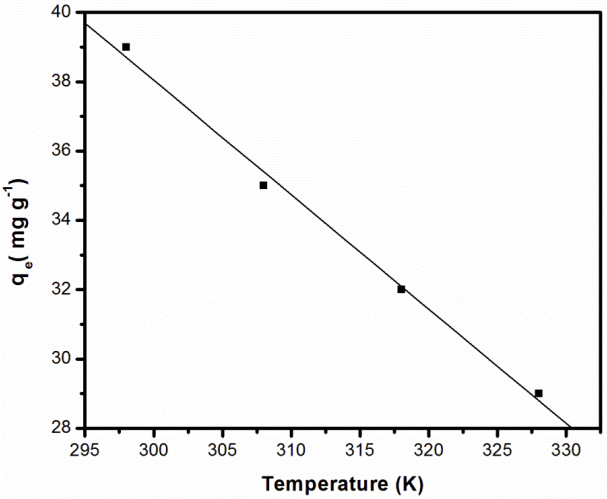

Fig. 6 Effect of temperature on the adsorption capacity of PANI/CeO_2-5 nanocomposite.

3.4. Adsorption isotherms

The equilibrium of adsorption is one of the important physicochemical aspects for the evaluation relationship between the quantity of adsorbate per unit of adsorbent (q_e) and its equilibrium solution concentration (C_e) at a constant-temperature was known as the adsorption isotherm. The distribution of solute between the solid and liquid phases is a measure of the distribution coefficient in the adsorption process and can be shown by the Freundlich and Langmuir equations.

The Langmuir adsorption [28] is based on the assumption that adsorption occurs at specific homogeneous sites within the adsorbent and once a dye molecule occupies a site, no further adsorption takes place at that site. Moreover, Langmuir's model of adsorption depends on the assumption of monolayer adsorption on a structurally homogeneous adsorbent, where all the sorption sites are identical and energetically equivalent. The intermolecular forces decrease rapidly with distance and can be used to predict the existence of monolayer coverage of the adsorbate at the outer surface of the adsorbent.

The Freundlich equilibrium isotherm [29] is used for the description of multilayer adsorption with interaction between adsorbed molecules. Model predicts that the dye concentrations on the material will increase as long as there is an increase of the dye concentration in the solution. Usually it applies to adsorption onto heterogeneous surfaces with a uniform energy distribution and reversible adsorption. The application of the Freundlich equation suggests that adsorption energy exponentially decreases on completion of the adsorption centers of an adsorbent. The linear form of Langmuir and Freundlich equations are represented mathematically by Eqs. (4) and (5), as follows:

$$C_e/q_e = 1/K_L.q_{max} + C_e/q_{max} \quad (4)$$

$$\ln q_e = \ln K_F + (1/n)\ln C_e \quad (5)$$

Where q_e is the amount of dye adsorbed at equilibrium (mg/g), q_{max} is the theoretical maximum monolayer sorption capacity (mg/g), and C_e is the equilibrium concentration of dye in solution (mg L^{-1}). K_L, K_F and n are empirical constants. K_L measures the affinity of the sorbent for the solute. K_F and n are constants that can be related to the adsorption capacity and the adsorption intensity, respectively. 1/n values indicate the type of isotherm to be irreversible (1/n = 0), favorable (0 <1/n < 1) and unfavorable (1/n >1) [30].

For the Langmuir-type adsorption process, the influence of the isotherm shape on whether adsorption is favorable or unfavorable can be classified by a dimensionless separation factor R_L, which is considered as a more reliable indicator of the adsorption capacity. This constant is given by the following [31]:

$$R_L = \frac{1}{1 + K_L C_0} \quad (6)$$

Where C_o is the initial dye concentration and K_L is the Langmuir adsorption constant (L/mg). The values of R_L indicate the shapes of isotherms to be either unfavorable (R_L> 1), linear (R_L= 1), favorable (0 < R_L< 1) or irreversible (R_L= 0). Favorable adsorption is reported when the R_L values are between 0 and 1.

The equilibrium adsorption data of dye onto PANI/CeO_2 adsorbents was analyzed using Langmuir and Freundlich models. The obtained experimental data were fitted with these two models; the resulting plots were shown respectively in Fig. 7 (a &b). Table 2 summaries the Langmuir and Freundlich isothermal parameters for the adsorption of dye on as-prepared PANI/CeO_2 nanocomposites. As shown in Table 2, the Langmuir and Freundlich isotherms were found to be linear over the whole concentration range studied with R^2> 0.98.In addition, the values of 1/n <1showed that the adsorption of the dye was favorable by Freundlich isotherm model (Table 2). It can also be observed that the values of q_{max} were higher than $q_{e\ (exp)}$, which confirmed the unfavorable uptake of the dye process by Langmuir isotherm model. So, the experimental equilibrium data were better described by Freundlich isotherm model indicating positive cooperativity in binding and a heterogeneous nature of adsorption.

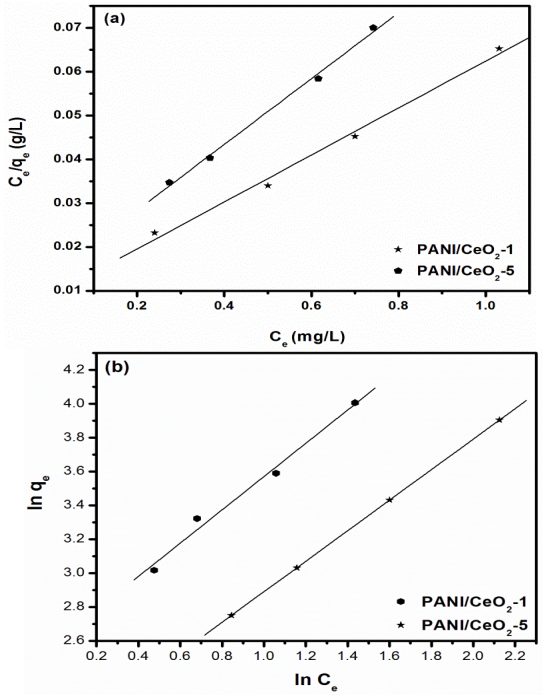

Fig. 7 Langmuir isotherms (a) and Freundlich isotherms (b) for Remazol Red RB-133 dye adsorption onto PANI/CeO_2 nanocomposites.

Table 2 Langmuir and Freundlich isotherm constants for Remazol Red RB-133 dye adsorption onto PANI/CeO_2 nanocomposites.

nanocomposites	**Langmuir isotherm model**				**Freundlich isotherm model**			
	q_{max} (mg/g)	K_L (L/mg)	R^2	R_L	K_F (mg/g)	n	1/n	R^2
PANI/CeO_2-1	18.6	6	0.992	0.24	13.3	1.02	0.98	0.99
PANI/CeO_2-5	13.9	5.6	0.996	0.26	7.3	1.11	0.90	0.999

3.4 Kinetics of Adsorption

The adsorption kinetics provides an idea about the mechanism of adsorption, from which efficiency of process estimated**.** Any adsorption procedure is ordinarily controlled by three dispersion steps: (i) transport of the solute from the bulk solution to the film surrounding the adsorbent, (ii) from the film to the adsorbent surface, (iii) from the surface to the inside targets took after by tying of the metal particles to the dynamic districts. The general rate of the adsorption procedure is directed by the slowest step and as a rule it is felt that the step (ii) prompts surface adsorption and the stride (iii) prompts intra-molecule adsorption [32]. The kinetics of Remazol Red RB-133 (RR RB-133) dye adsorption onto 0.1 g of PANI/CeO_2 nanocomposites and pure PANI acquired by batch contact time studies for a dye concentration of 50 mg L^{-1} at pH 6.5 were demonstrated in Fig. 8. The results revealed that adsorption procedure was obviously time dependent such that the dominant part of the dye adsorption from aqueous solution was finished in more or less 1.5 h. Also, under the same experimental conditions utilized, PANI/CeO_2 nanocomposites have much faster dye uptake rate and higher adsorption capacity than that of pure PANI adsorbent. It is noticed that CeO_2 loading accelerated the adsorption process. PANI/CeO_2-5 adsorbent reached about 99% of the adsorption capacity in almost half the time as pure PANI, because of the high solid/liquid interface and upgraded adsorption sites. It must be identified by their higher particular surface regions and smaller pore width and also exceptional microporous structures. The removal efficiencies of dye within 40 min were ranked as: PANI/CeO_2-5>PANI/CeO_2-1>pure PANI. In order to assess the kinetic mechanism which controls the adsorption process, the pseudo-first-order [34], pseudo-second order [35], and intraparticle diffusion [36] models were examined, and the validity of the models were confirmed by the linear equation analysis log ($q_e - q_t$) vs. t, (t/q_t) vs. t, and q_t vs. $t_{1/2}$, separately. Great relationship with the kinetic data clarifies the dye adsorption mechanism on the polyaniline composite.

The first model is pseudo-first order and can be represented by the following form [33]:

$$\ln(q_e - q_t) = \ln q_e - k_1 t \qquad (7)$$

Where q_e and q_t are the amounts of dye adsorbed (mg/g) at equilibrium and at time t (min), individually, and k_1 (min^{-1}) is the pseudo-first-order rate constant. Values of k_1 are obtained from the plots of ln (q_e–q_t) versus t (see Fig. 9a) for the four composite specimens. The correlation coefficient R^2 values were not higher than 0.98 and the experimental q_e values demonstrated a good agreement with the calculated values from the direct plots (Table 3), showing the suitability of this model to

represent the adsorption procedure of dye onto the PANI/CeO_2 nanocomposites and pure PANI.

The second model, the pseudo-second-order reaction, is dependent on the amount of solute adsorbed on the surface of the adsorbent and the amount adsorbed at equilibrium. It can be described in the following form [34]

$$t/q_t = 1/k_2 q_e^2 + t/q_e \quad (8)$$

Fig. 9b shows the curve-fitting plots of Equation 8 ((t/q_t) vs. t), and the parameter values of q_e, k_2 and R^2 were determined and listed in Table 3. From which it can be seen that the pseudo-second-order kinetic model showed a better coefficient correlation for the adsorption of dye onto the PANI/CeO_2 nanocomposites and pure PANI compared to the pseudo-first-order model. Moreover, the calculated values of q_e for pseudo-second-order model are in good agreement with the experimental values of q_e which indicates that the rate-limiting step may be chemisorption and that the rate equation follows second-order kinetics.

The third model is an intraparticle diffusion model. It is proposed by Weber and Morris [35] and stated that if intraparticle diffusion is the rate-controlling factor, uptake of the adsorbate varies with the square root of time and is expressed by Equation 9:

$$q_t = k_{dif}\sqrt{t} + C \quad (9)$$

Where $k_{dif}$is the intraparticle diffusion rate constant ($mg/gmin^{1/2}$) and C is the intercept related to the thickness of the boundary layer. The plots of q_t versus $t^{1/2}$, shown in Fig. 9c, would realize a straight relationship and k_{dif} and C values obtained from these plots were recorded in Table 3. Fig. 9c also shows that there are two different stages: a linear stage and a non-linear stage, which indicates more than one process is involved in the dye sorption process. The beginning stage in diffusion model is the mass exchange of adsorbate molecule from the mass reaction to the adsorbent surface and the second stage is attributed to the intraparticle pore diffusion effect.

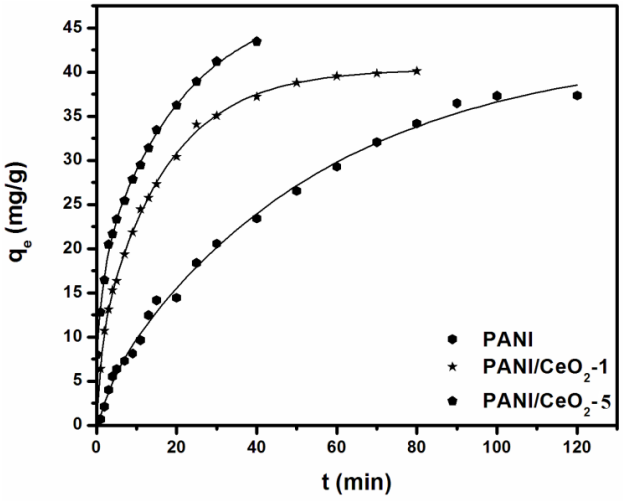

Fig. 8 The variation in adsorption capacity with adsorption time for Remazol Red RB- 133 dye onto PANI and PANI/CeO_2 nanocomposites (dye concentration is 50 mg L^{-1}, adsorbent dosage = 0.1 g L^{-1}, pH = 6.5).

Table 3 Fitted kinetics parameters for the adsorption of Remazol Red RB-133 dye on pure PANI and PANI/CeO_2 nanocomposites (dye: 50 mg/L; pH: 6.5; 0.1 g)..

Intra-particle diffusion						Pseudo-second-order model			Pseudo-first-order model			$q_{e,exp}$ (mg/g)	Samples
R_2^2	C_2	k_{dif2} (mg/min^{½} g)	R_1^2	C_1	k_{dif1} (mg/min^{½} g)	R^2	k_2 (g/mg min)	$q_{e,cal}$ (mg/g)	R^2	k_1 (min^{-1})	$q_{e,cal}$ (mg/g)		
0.62	33.5	0.52	0.99	-1.77	4.25	0.98	5.22 x10^{-4}	40	0.93	0.033	40.5	36	PANI
0.93	29.9	1.04	0.99	-1.04	6.84	0.99	8.75 x10^{-4}	43	0.98	0.072	34.8	37.8	PANI/CeO_2-1
0.97	18.4	3.87	0.99	6.39	6.78	0.99	2.61 x10^{-3}	43.3	0.98	0.11	30	38.7	PANI/CeO_2-5

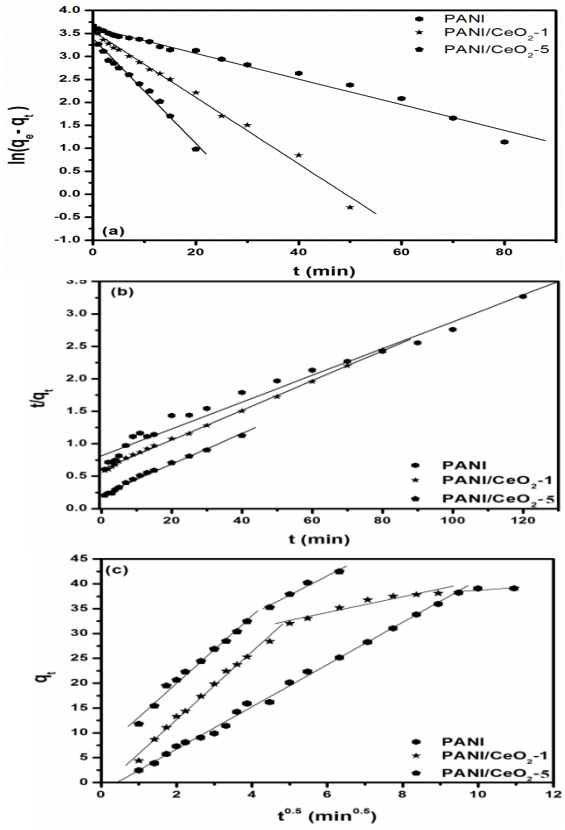

Fig. 9 Pseudo-first-order kinetics (a), second-order kinetics (b) and intra-particle diffusion kinetics (c) for Remazol Red RB-133 dye adsorption onto PANI and PANI/CeO_2 nanocomposites (dye concentration is 50 mg L^{-1}, adsorbent dosage = 0.1 g L^{-1}, pH = 6.5).

3.5. Adsorption thermodynamic

The energy and entropy considerations were very important in order to understand the kinetics of adsorption. Thermodynamic parameters such as standard enthalpy change (ΔH^o) and standard entropy change (ΔS^o) were determined from the slope and intercept of Van't Hoff's plot of ln K_c versus 1/T (Equation 10) [36, 37].

$$\ln K_c = \ln\left({}^{q_e}/_{C_e}\right) = -\,{}^{\Delta H^o}/_{RT} + {}^{\Delta S^o}/_{R} \qquad (10)$$

where K_c is the equilibrium constant, (q_e/C_e) is the adsorption distribution coefficient, (ΔH^o) is the standard enthalpy change (kJ mol^{-1}), (ΔS^o) is standard entropy change (kJ mol^{-1} K^{-1}), T is the temperature in Kelvin and R is the universal gas constant (8.314 J/ mol K).

The change in free energy of sorption (ΔG^o) is calculated by

$$\Delta G^o = \Delta H^o - T\Delta S^o \qquad (11)$$

The calculated values of thermodynamic parameters are shown in Table 4. The negative values of ΔH^o The negative value of entropy change (ΔS^o) corresponds to a decrease in degree of freedom of the adsorbed species. This suggests the decrease in concentration of adsorbate in solid–solution interface, indicating there by an increase in adsorbate concentration on the solid phase. This is the normal effect of chemical adsorption phenomenon, which takes place through ion-exchange interactions [39]. In order to further confirm that chemisorption is the predominant mechanism, the values of activation energy (E_a) and sticking probability (S*) were calculated using a modified Arrhenius type equation related to surface coverage (θ) as follows:

$$S^* = (1 - \theta)\, e^{-E_a/RT} \qquad (12)$$

The S* is a function of the adsorbate/adsorbent system under investigation, its value lies in the extent 0 <S*< 1 and is a subject to the temperature of the system. The value of θ can be calculated from the following equation:

$$\theta = \left[1 - {}^{C_e}/_{C_0}\right] \qquad (13)$$

The E_a was calculated from the slope of the plot of ln (1- θ) vs. 1/T (Fig. 10b). The magnitude of activation energy gives an idea regarding the type of adsorption, which is predominantly physical or chemical. The physisorption frames as a general rule have energies in the extent of 5–40 kJ/mol, while higher activation energies (40–800 kJ/mol) propose chemisorption [38]. The value of E_a for the adsorption of Remazol Red RB-133 on PANI/CeO_2-5 nanocomposite was observed to be 55.17 kJ/mol, and this suggesting that chemisorption was the predominant mechanism involved.

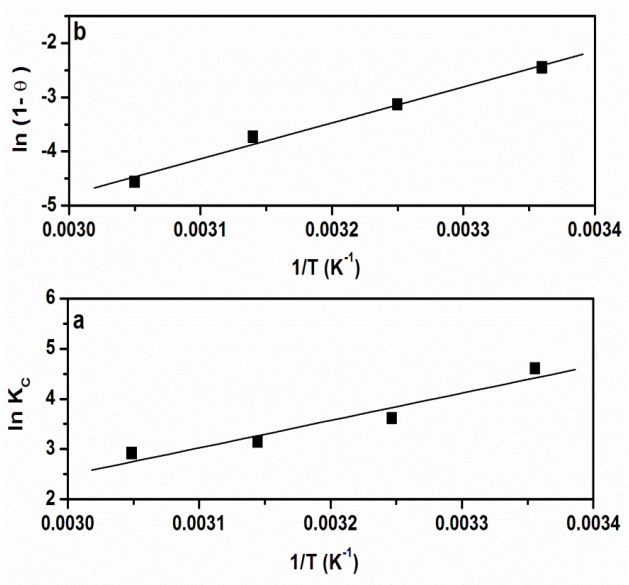

Fig. 10 (a) Van't Hoff plot and (b) modified Arrhenius plot for the adsorption of Remazol Red RB-133 dye onto PANI/CeO_2-5 nanocomposite.

Table 4 Thermodynamic parameters for the adsorption of Remazol Red RB-133 dye (50 mg/L) on PANI/CeO_2-5 nanocomposite at pH 6.5.

Temperature (°C)	ΔG° (kJmol^{-1})	ΔS° (JK^{-1}mol^{-1})	ΔH° (kJ mol^{-1})	K_c	E_a (kJ mol^{-1})	S*
25	-10.94	-115.24	-45.29	99.37	55.17	1.85×10^{-11}
35	-9.79			36.87		
45	-8.64			23.05		
55	-7.49			18.41		

4. Conclusions

The pure PANI, PANI/CeO_2 nanocomposites (1 and 5 wt% CeO_2) were prepared from aniline in the presence of an oxidizing agent via in situ polymerization method. Introducing CeO_2 into the polymeric matrix significantly improved the surface and adsorptive properties of PANI. The composite samples showed better adsorption efficiency for removing RR RB- 133 acid dye from an aqueous solution than that of pure PANI. Adsorption rate increases in the following order: PANI/CeO_2-5>PANI/CeO_2-1> pure PANI. This is possibly because of the increase in the surface area of polymer. The adsorption kinetics can be successfully fitted to pseudo-second-order kinetic model. Adsorption parameters for the Langmuir and Freundlich isotherms were determined and the equilibrium data were best described by the Freundlich isotherm model. The adsorption of the acid dye at various temperatures shows that the adsorption is spontaneous, endothermic and marked with an increased randomness at the solid–liquid interface. The present study suggested that conducting PANI/CeO_2 can be used as a potential adsorbent for the removal of acidic dyes from aqueous solutions.

5. References

[1] K.Y. Foo, B.H. Hameed, Chemical Engineering Journal 156 (2010) 2–10.

[2] A. M. Donia, A. A. Atia , W. A. Al-amrani, A. M. El-Nahas, Journal of Hazardous Materials 161 (2009) 1544–1550.

[3] A.R. Cestri, E.F.S. Vieira, A.A. Pinto, E.C.N. Lopes, J. Colloid Interf. Sci. 292 (2005) 363–372.

[4] A. Krysztafkiewicz, S. Binkowski, T. Jesionowski, Appl. Surf. Sci. 199 (2002) 31–39.

[[5] K.C. Chen, J.Y. Wu, C.C. Huang, Y.M. Liang, S.C.J. Hwang, Journal of Biotechnology 101 (2003) 241–252.

[6] T. Robinson, G. McMullan, R. Marchant, P. Nigam, Remediation of dyes in textile effluent: a critical review on current treatment technologies with a proposed alternative, Biosour. Technol. 77 (2001) 247–255.

[7] T. Jesionowski, Dyes and Pigments 55 (2002) 133–141.

[8] E. Eren, B. Afsin, Dyes and Pigments 76 (2008) 220–225.

[9] A.R. Cestari, E.F.S. Vieira, G.S. Vieira, L.E. Almeida, J. Hazard. Mater. B 138 (2006) 133–141.

[10]Y.C. Sharma, S.N. Uma, G.F. Upadhyay, J. of Applied Science in Environmental Sanitation 4 (2009) 21–24.

[11] A. Khenifi , Z. Bouberka , F. Sekrane, M. Kameche, Z. Derriche, Adsorption 13 (2007) 149–158.

[12] R. C. Torane, K. S. Mundhe, A. A. Bhave, G. S. Kamble, R. V. Kashalkar, N. R. Deshpande, Der Pharma Chemica 2 (2010) 171–177.

[13] D. Bingola, S. Veli, S. Zora, U. Ozdemirb, Synth. Met. 162 (2012) 1566 –1571.

[14] S. C. Kuiry, S. Patil, S. Deshpande, S. Seal, J. Phys.Chem. B 109 (2005) 6936-6939.

[15] T. N. Ravishankar, T. Ramakrishnappa, G. Nagaraju, H. Rajanaika, Chemistry Open 4 (2015) 146–154.

[16] A.G. Macdiarmid, J.C. Chiang, A.F. Richter, A.J. Epstein, Synthetic Met. 18 (1987) 285–290.

[17] *F. Y. Chuang, S. M. Yang*, J Colloid Interface Sci. 320 (2008) 194–201.

[18] B. D. Cullity, Addison-Wesley, Reading, Mass, USA, 3rd edition, 1967.

[19] T. Abdiryim, Z. Xiao-Gang, R. Jamal, Mater Chem Phys 90 (2005) 367–372.

[20] E. Kumar, P. Selvarajan, D. Muthuraj, J Mater Sci 47 (2012) 7148–7156.

[21] M. M. Ayad, A. Abu El-Nasr, J. Stejska, Journal of Industrial and Engineering Chemistry 18 (2012) 1964–1969.

[22] Z. L. Wang, X. Feng, *Phys. Chem. B 107* **(2003)** 13563–13566.

[23] S. Brunauer, P.H. Emmett, E. Teller, J.Am. Chem. Soc. 60 (1938) 309–319.

[24] R. Karthik, S. Meenakshi, Journal of Water Process Engineering 1 (2014) 37–45.

[25] M. Anbia, S. Salehi, Dyes and Pigments 94 (2012) 1–9.

[26] S. Mandal, S.S. Mahapatra, R.K. Patel, Journal of Environmental Chemical Engineering 3 (2015) 870–885.

[27] Y. S. Ho, J. C. Y Ng., G. Mckay, Separ.Purif. Method. 29 (2000) 189–191.

[28] I. Langmuir, *Journal of the American Chemical Society 40 (1918) 1361–1403.*

[29] H. M. F.Freundlich, J. Phys. Chem. 57 (1906) 385-470.

[30] H. Zhang, Y. Tang, D. Cai, X. Liu, X. Wang, Q. Huang, Z. Yu, J. Hazard. Mater. 181 (2010) 801–808

[31] T. W. Weber, R. K.Chakravorti, Journal of American Institute of Chemical Engineering 20 (1974) 228–238.

[32] Y. S. Ho, J. C.Y. Ng , G. McKay, Separation and purification methods 29 (2000) 189–232.

[33] G. McKay, Y. S. Ho, Process Biochem. 34 (1999) 451–465.

[34] W. J. Weber, J. C. Morris, Pergamon, Oxford, 2 (1962) 231–266.

[35] Y. Wang, X. Wang, J. Li, Z. Mo, X. Zhao, X. Jing, F. Wang, Adv. Mater. 13 (2001) 1582–1585.

[36] S. Fedorova, J. Stejskal, Langmuir 18 (2002) 5630–5632.

[37] M. Ghaedi, A. Hekmati Jah, S. Khodadoust, R. Sahraei, A. Daneshfar, A. Mihandoost, M.K. Purkait, Spectrochimica Acta, Part A 90 (2012) 22–27.

[38] A. Özcan, E. M. Öncü, A. S. Özcan, Colloids and Surfaces A: Physicochemical and Engineering Aspects, 277 (2006) 90-97.